



Analysis on Surface Deformation and Cracks in Paddy Fields by 2016 Kumamoto Earthquake using GNSS and Photogrammetry

TAKAHIKO KUBODERA*

*Faculty of Science and Engineering, Toyo University, Saitama, Japan
Email: kubodera@toyo.jp*

TAKANOBU SUZUKI

Faculty of Science and Engineering, Toyo University, Saitama, Japan

HIROSHI MASAHARU

Faculty of Science and Engineering, Toyo University, Saitama, Japan

EIJI MATSUO

Faculty of Engineering, Kyushu Sangyo University, Fukuoka, Japan

Received 10 January 2017 Accepted 5 May 2017 (*Corresponding Author)

Abstract Paddy fields in Kumamoto Prefecture were struck seriously by the 2016 Kumamoto Earthquake. The surface deformation and cracks damaged water distribution system for paddy fields. In order to clarify damages with rapidity, the surveying combining the aerial-based surveying and ground-based surveying was necessary. The aerial photogrammetry was conducted for the surface deformation and crack area, to clarify them quantitatively. The aerial photos were taken by an airplanes after the earthquakes. The aerial photogrammetry by airplane is suited to compare the topographic model after earthquakes to the topographic model before earthquakes, because the topographic model before earthquakes was surveyed by airplane. The Global Navigation Satellite System (GNSS) surveying was also conducted at the ground points in the area of aerial photos. The orthophoto mosaic and the Digital Elevation Model (DEM) after the earthquakes were made from these surveying. Further, the orthophoto mosaic and the DEM after the earthquakes were input into the Geographic Information System (GIS), to analyze the surface deformation and cracks in paddy fields. The accurate positions for cracks were found by overlaying the translucent orthophoto mosaic on the existing map. The differences between the DEMs before and after the earthquakes were analyzed by overlaying the DEM after the earthquakes on the DEM before the earthquakes. As the results, it was found that the overall upheaval and the local cave-in arose in the focused paddy field. The overall upheaval was 0.0 m - 0.4 m. The local cave-in was about 2.0 m. In order to check the differences between the DEMs before and after the earthquakes, the DEM after the earthquakes was compared to the elevation value by the GNSS surveying at the verification points. As the result, it was verified that the difference was 0.118 m as standard deviation.

Keywords aerial photogrammetry, GNSS, DEM, GIS, paddy field

INTRODUCTION

The Kumamoto Earthquake was a series of earthquakes that struck Kumamoto Prefecture in the south of Japan on and after April 14, 2016. A foreshock with a magnitude on the Japan Meteorological Agency seismic intensity scale of Mj 6.5 and with its hypocenter at a depth of 11 km struck the

Kumamoto area at 9:16 p.m. on April 14, 2016. At 1:25 a.m. on April 16, 28 h after the foreshock occurred, the main shock with a magnitude of Mj 7.3 and with its hypocenter at a depth of 12 km struck the same Kumamoto area that had experienced the foreshock (Kato et al., 2016). Kumamoto Prefecture is highly productive in terms of agriculture, as evidenced by the fact that, before the earthquakes occurred, it was ranked the fifth most productive prefecture out of all the 47 prefectures in Japan in terms of the value of agricultural production. However, after the earthquakes, many paddy fields were seriously damaged because the vertical deformation and cracks made it impossible to irrigate them.

In this study, we conducted aerial photogrammetry and a Global Navigation Satellite System (GNSS) survey, because a survey consisting of both aerial- and ground-based studies were necessary for a prompt understanding of the complete picture of the damaged area. Aerial photogrammetry is a surveying technology utilizing ground-based three dimension (3D) models, which are constructed from photos taken from the sky, camera coordinate values, and coordinate values of ground control points (GCPs). In this study, we also built digital elevation models (DEMs) and orthophoto mosaics, because these were obtainable through the aerial photogrammetry. DEMs are models of the elevations of the land surface, excluding the heights of buildings and vegetation. An orthophoto mosaic is a single aerial photograph on which several orthographically projected aerial photographs are assembled. We conducted the GNSS surveying of the devastated areas to obtain the coordinate values of the GCPs. A GNSS surveying is a survey method to determine the positions using signals from positioning satellites such as the GPS, GLONASS and Galileo. The accuracy ranges from several meters to several millimeters, depending on the method used. In this research, we conducted a network-based real time kinematic (RTK) GNSS surveying to determine the coordinate values of the GCPs with high accuracy of several millimeters. We used the Geographic Information System (GIS) to determine the difference between the DEMs before and after the earthquakes in order to clarify the vertical deformation of the land surface in the paddy fields quantitatively.

The satellites have been used for surveying in Kumamoto (Research Group for High-resolution Satellite Remote Sensing, 2016; Obata and Iwao, 2016). The drones have been used for surveying in Kumamoto (Ishiguro et al., 2016). In this research, we considered that aerial photogrammetry by airplane would be preferable to satellite or drone for the comparison of the DEMs before and after the earthquakes, because an airplane survey had already been conducted to obtain a DEM before the earthquakes. For this reason, we used aerial photos taken from an airplane after the earthquakes. In Japan, the Geospatial Information Authority of Japan (GSI) has built a detailed database of the country's land surface with airplanes, and it released the DEM before the earthquakes free of charge. We used aerial photogrammetry to build the DEM after the earthquakes, and analyzed the difference between the DEMs before and after the earthquakes. At the same time, we overlaid orthophoto mosaics we built from the aerial photogrammetry onto the existing maps to determine cracks on the land surface in the paddy fields.

METHODOLOGY

Figure 1 shows the target area of the survey and analysis. Kumamoto Prefecture is located in the southern part of Japan. Of the large area damaged by the earthquakes, we selected Aso City in order to focus on the damage to paddy fields. We used the photogrammetry software PhotoScan Professional, which is a structure-from-motion (SfM) software product. PhotoScan Professional allows for aerial triangulation with the help of multiple aerial photos and multiple GCPs. It creates DEMs through image matching and filtering treatments, and also creates orthophoto mosaics automatically. Fig. 2 shows the 3D model that we created. The blue rectangles in the sky show the 3D position and attitude of the aerial photographs. The circles on the land surface indicate the 3D positions of the GCPs where we conducted the GNSS surveying. The coordinate system we used is the Japanese Geodetic Datum

(JGD) 2011 Plane-rectangular Coordinate System Area 2 (Matsumura et al., 2004; Tsuji and Matsuzaka, 2004; Imakiire and Hakoiva, 2004; Geospatial Information Authority of Japan, 2011). We successfully created a group of 3D points on the land surface through aerial photogrammetry. On the near side of the Fig. 2, the site of the landside disaster triggered by the earthquakes can be seen. The aerial photographs were taken on July 5, 2016. The digital aerial camera provides its orientation accurately because it was calibrated. Using the RTK GNSS surveying and Inertial Measurement Unit (IMU) technology, it was possible to provide the coordinate axes and attitudes of the digital aerial camera with high accuracy of several tens of millimeters.



Fig. 1 Target area in Kumamoto

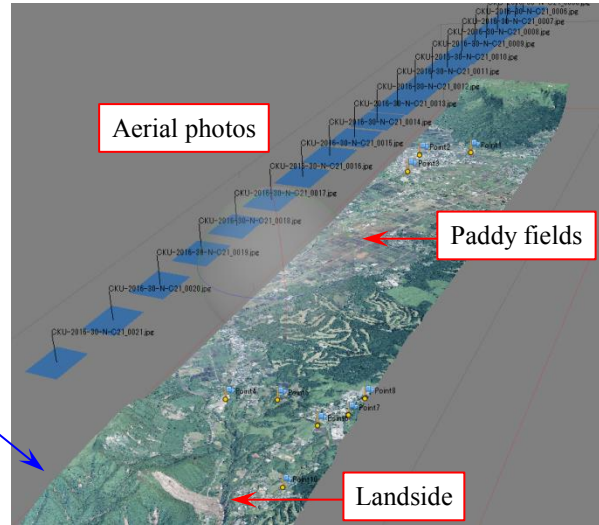


Fig. 2 The 3D model by aerial photogrammetry



Fig. 3 GNSS surveying

Table 1 SD values of residual errors of the most probable values of nine GCPs

	X [m]	Y [m]	H [m]
SD	0.088	0.149	0.149

As the photograph in Fig. 3 shows, we conducted a network-based RTK GNSS surveying in Kumamoto on the 23rd and 24th of July 2016. We used the Trimble R10 for the GNSS surveying, and three types of satellite: GPS, GLONASS, and the Quasi-Zenith Satellite System (QZSS). In addition, we used two frequency bands: L1 and L2. The geoid model we used was “GSIGEO2011” (Miyahara et al., 2014; Kubodera et al., 2016). For conducting the GNSS surveying on the ground, we selected the four corners of the course, sites accessible by car, and pavements so that the aerial camera could take clear photographs. Based on the surveying calculations from the GNSS surveying, we found that the standard deviation (SD) of the most probable value was less than 0.01 m. We conducted aerial

triangulation based on the 3D coordinate values of the camera and the GCPs. Table 1 shows the SD values of residual errors of the most probable values of nine GCPs. The SD values for the X and Y coordinates and elevation H were lower than 0.15 m, indicating a high accuracy. We created a DEM after the earthquakes with 1 m mesh, in order to determine the differences between the DEMs before and after the earthquakes as well as the elevation values. In addition, we created orthophoto mosaics to gain a clearer picture of the damage.

RESULTS AND DISCUSSION

Specifying the Position of Cracks with Orthophoto Mosaic

Figure 4 shows the orthophoto mosaic developed on the GIS. For the aerial photogrammetry, we used the JGD2011 Plane-rectangular Coordinate System Area 2. The GIS software used was ArcGIS 10.4.1. We used the existing map as a background for confirmation of the positions. By doing this, we found that the created mosaic was developed on the designated positions correctly. The orthophoto mosaic indicates that this area consists of paddy fields. Subsequently, we set the transmission of the orthophoto mosaic at 50% and overlaid it onto the existing map to specify the positions of cave-ins. As shown in Fig. 5, we successfully specified the exact positions of the cracks. We were able to confirm cracks along the fault that occurred in the paddy fields. Fig. 6 shows a photograph taken by the second author of this study immediately after the earthquakes occurred in the area surrounding the paddy fields. It shows several cracks created along the fault. This visually confirms that there was a cave-in about 2 m deep.

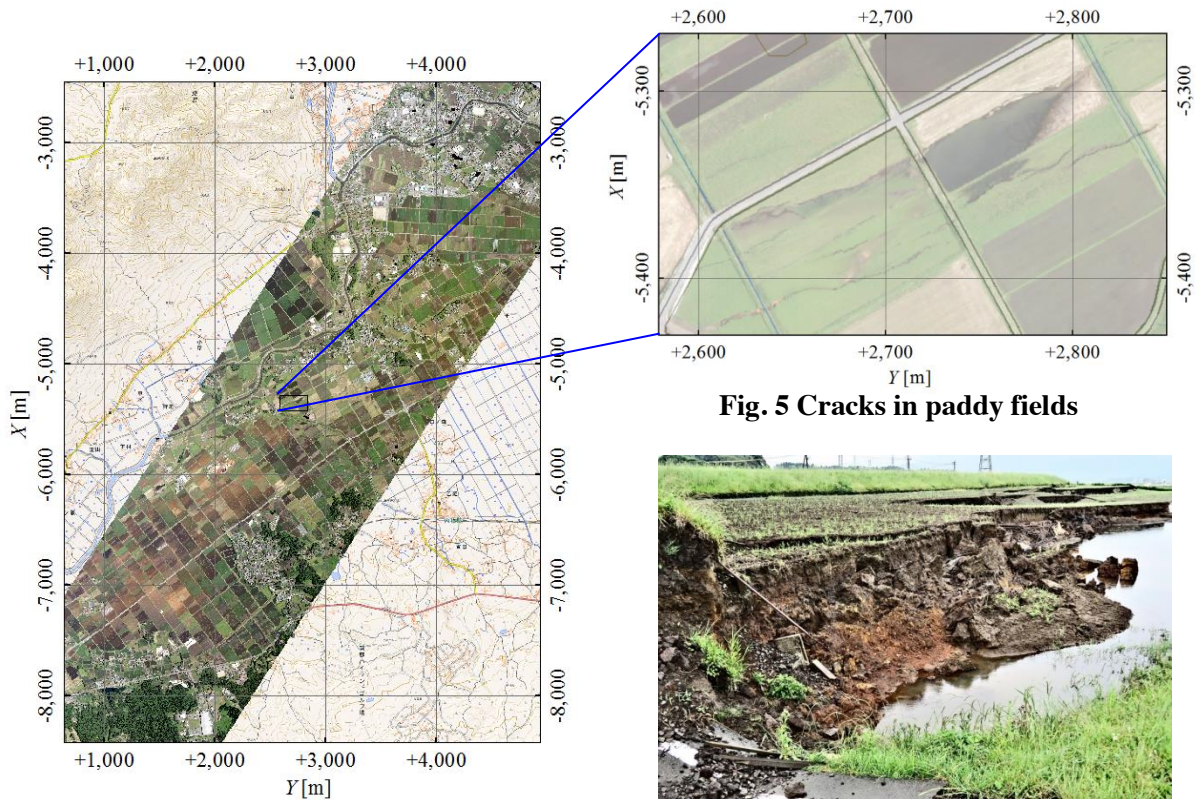


Fig. 4 Orthophoto mosaic developed on the GIS



Fig. 6 Actual cracks

Differences between the DEMs before and after the Earthquakes

For the DEM before the earthquakes, we used the results (5 m mesh, elevation value in units of 0.01 m) obtained from the GSI. For the analysis of the difference between the DEMs before and after the earthquakes, we set the mesh sizes of the DEM before and after the earthquakes to 1 m. Fig. 7 shows the results of the analysis. We deducted the elevation values of the DEM before the earthquakes from those of the DEM after the earthquakes to obtain the differences. We blacked out the objects with a height difference greater than 3 m because these were assumed to be vegetation or buildings. The analysis results indicate that the area on which we focused underwent upheaval as a whole. When focusing on the agricultural roads, it was found that they underwent upheaval of 0.0–0.4 m. The paddy fields apparently underwent greater upheaval than the agricultural roads, but ambiguous places such as vegetation showed a low accuracy in matching. The rectangular part in the center of Fig. 7 is the cracked part shown in Fig. 5. Based on the analysis of the differences between the DEMs before and after the earthquakes, we successfully clarified the vertical deformation both dimensionally and quantitatively.

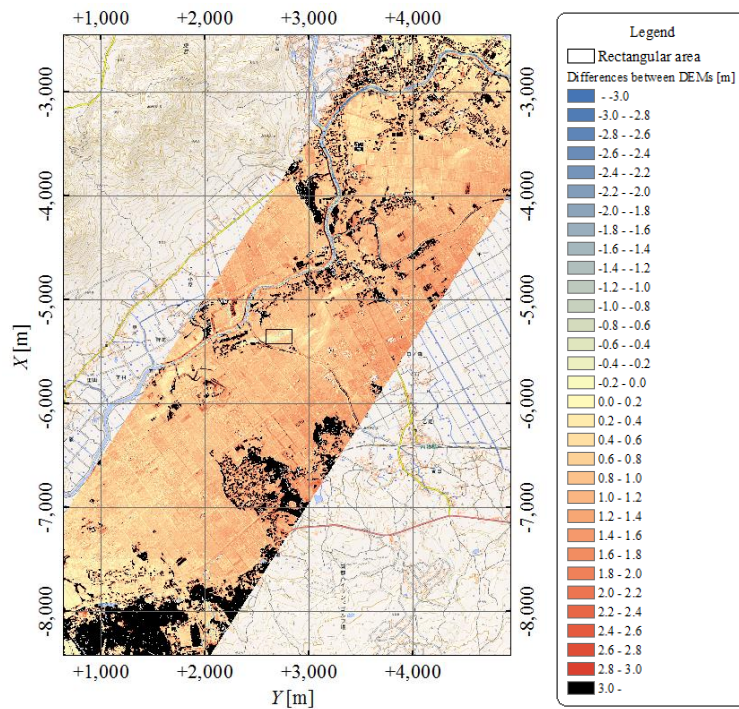


Fig. 7 Differences between the DEMs before and after the earthquakes

Accuracy Verification of Elevation Values

As Table 2 shows, we compared the elevation values of the DEM after the earthquakes and those of the GNSS after the earthquakes at verification points to verify the accuracy of the constructed DEM after the earthquakes. At these verification points, we did not adopt the GCPs by aerial triangulation, but rather conducted a GNSS surveying on the points. The GNSS showed a higher accuracy than the DEM. Based on the above results, we found that the elevation values of the DEM and the GNSS after the earthquakes closely matched each other with the discrepancies between them ranging from +0.031 m to +0.196 m. The SD of the elevation values of the DEM after the earthquakes was 0.118 m, assuming

that the elevation values of the GNSS after the earthquakes were true values. That is, it is possible to state that the DEMs after the earthquakes was accurate with an SD of 0.118 m.

Table 2 Accuracy verification of elevation values

Name of point	Elevation value [m]		
	DEM after earthquake	GNSS after earthquake	Discrepancy
1	482.608	482.577	+0.031
2	479.938	479.888	+0.050
3	478.280	478.084	+0.196
		SD	0.118

Comparison of the DEMs before and after the Earthquakes with the Lateral Profile

We found several points where a cave-in could be confirmed by the orthophoto mosaic of Fig. 5, even though it was not possible to detect these when comparing the differences between the DEMs before and after the earthquakes, such as in the rectangle in Fig. 7. The reason for this may be that, although the point caved-in, it underwent upheaval as a whole. For this reason, we compared the DEMs before and after the earthquakes using a lateral profile. Fig. 8 shows the transverse line A–A’ used to compare the DEMs before and after the earthquakes. We designated Points B, C, D, E, and F at distances of 4, 20, 30, 60, and 70 m from Point A. This rectangular area is the same as that shown in Fig. 5. Although the earthquakes caused a cave-in, a large difference could not be detected when comparing the DEMs before and after the earthquakes. This is presumably because the overall area underwent upheaval, thus causing a relative cave-in. Fig. 9 shows a cross section along the line A–A’. The section from Point A to Point B is a paved agricultural road, and it underwent upheaval of about 0.9 m as a result of the earthquakes. This upheaval can be observed from Points A to C. However, a sharp cave-in from the level before the earthquakes can be detected from Points C to E. At Point D, where the sharpest cave-in was observed, the height difference was about 2 m from the land surface. It could also be determined that upheaval resumed from Points F to A’. When comparing the DEMs before and after the earthquakes, it was found that the paddy fields had a more irregular elevation profile on the DEM after the earthquakes. This is presumably because the image mapping has a low accuracy in areas with vegetation. As a whole, we successfully clarified the vertical deformation of the cracks on the fault dimensionally and quantitatively.

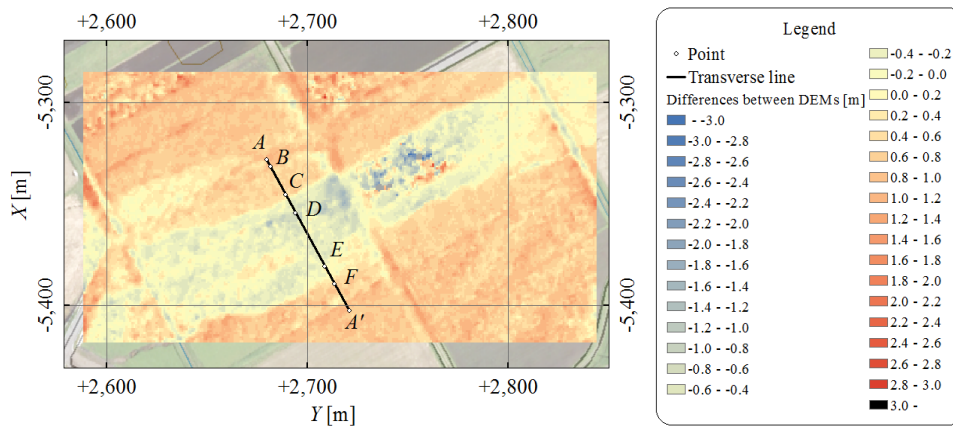


Fig. 8 Differences between the DEMs before and after the earthquakes at the cracks

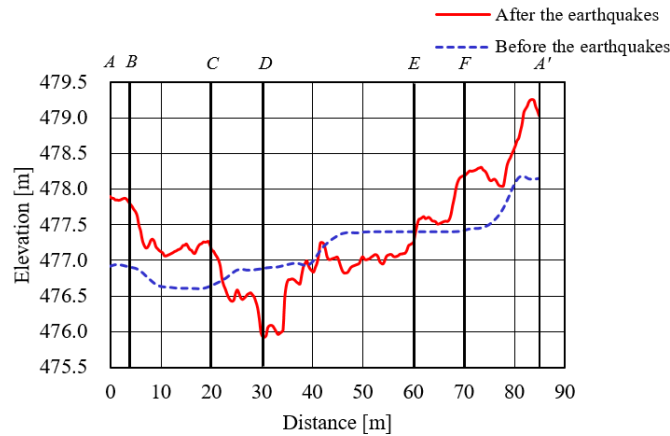


Fig. 9 Cross section at the cracks

CONCLUSION

As the conclusions, the following points are summarized in this study.

- (1) The exact positions of the cracks in paddy fields were specified by the orthophoto mosaic.
- (2) Based on the analysis of the differences between the DEMs before and after the earthquakes, the vertical deformation was clarified dimensionally and quantitatively.
- (3) The SD of the elevation values of the DEM after the earthquakes was 0.118 m, assuming that the elevation values of the GNSS after the earthquakes were true values. That is, it is possible to state that the DEMs after the earthquakes was accurate with an SD of 0.118 m.

ACKNOWLEDGEMENTS

The Information Provision Support Team of the Major Disaster Management Headquarters of GSI provided the aerial photos used in this research in order to support the recovery project implemented by Kumamoto Prefecture. We gratefully acknowledge the kindness and support they extended to our study.

REFERENCES

- Geospatial Information Authority of Japan. 2011. (Website: http://www.gsi.go.jp/ENGLISH/page_e30030.html, accessed; 15 Dec. 2016).
- Imakiire, T. and Hakoïwa, E. 2004. JGD2000 (vertical) -The New Height System of Japan-. Bulletin of the GSI, 51, 31-51.
- Ishiguro, S., Matsuta, N., Inoue, H., Nakata, T., Tanaka, K., Ishiyama, T., Mita, T., Takenami, D., Moriki, H. and Hirouchi, D. 2016. High-resolution digital surface models of surface rupture associated with the 2016 Kumamoto earthquake, by using unmanned aerial vehicle photography. Journal of The Remote Sensing Society of Japan, 36 (3), 214-217 (in Japanese).
- Kato, A., Nakamura, K. and Hiyama, Y. 2016. The 2016 Kumamoto earthquake sequence. Proceedings of the Japan Academy, Series B, 92 (8), 358-371.
- Kubodera, T., Okazawa, H., Hosokawa, Y., Kawana, F., Matsuo, E. and Mihara, M. 2016. Effects of surveying methods between GNSS and direct leveling on elevation values over long distance in mountainous Area. International Journal of Environmental and Rural Development, 7 (1), 62-69.
- Matsumura, S., Murakami, M. and Imakiire, T. 2004. Concept of the new Japanese Geodetic System. Bulletin of the GSI, 51, 1-9.

- Miyahara, B., Kodama, T. and Kuroishi, Y. 2014. Development of new hybrid geoid model for Japan, “GSIGEO2011”. Bulletin of the GSI, 62, 11-20.
- Obata, K. and Iwao, K. 2016. Relation between slope failures caused by Kumamoto earthquake in 2016 and NDVI changes in ASTER data. Journal of The Remote Sensing Society of Japan, 36 (4), 417-420 (in Japanese).
- Research Group for High-resolution Satellite Remote Sensing. 2016. High resolution satellite remote sensing for the disaster of the 2016 Kumamoto earthquake. Journal of The Remote Sensing Society of Japan, 36 (3), 211-213 (in Japanese).
- Tsuji, H. and Matsuzaka, S. 2004. Realization of horizontal geodetic coordinates 2000. Bulletin of the GSI, 51, 11-30.